CARBON letters

Original Articles
Carbon Letters Vol. 18, 37-42 (2016)

Atmospheric chemical vapor deposition of graphene on molybdenum foil at different growth temperatures

Samira Naghdi[1,2], Kyong Yop Rhee[2,♠], Man Tae Kim[3], Babak Jaleh[1] and Soo Jin Park[4,♠]

[1]Department of Physics, Bu-Ali Sina University, Hamedan 65174, Iran
[2]Department of Mechanical Engineering, College of Engineering, Kyung Hee University, Yongin 17104, Korea
[3]Airworthiness Certification Team, Defense Agency for Technology and Quality, Jinju 52851, Korea
[4]Department of Chemistry, College of Natural Science, Inha University, Incheon 22212, Korea

Article Info

Received 4 January 2016
Accepted 14 March 2016

***Corresponding Author**
E-mail: rheeky@khu.ac.kr
sjpark@inha.ac.kr
Tel: +82-31-201-2565
Tel: +82-32-876-7234

Open Access

DOI: http://dx.doi.org/10.5714/CL.2016.18.037

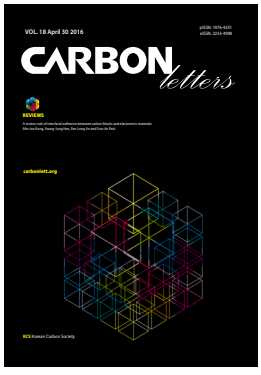

http://carbonlett.org

pISSN: 1976-4251
eISSN: 2233-4998

Abstract

Graphene was grown on molybdenum (Mo) foil by a chemical vapor deposition method at different growth temperatures (1000°C, 1100°C, and 1200°C). The properties of graphene were investigated by X-ray diffraction (XRD), X-ray photoelectron spectroscopy, and Raman spectroscopy. The results showed that the quality of the deposited graphene layer was affected by the growth temperature. XRD results showed the presence of a carbide phase on the Mo surface; the presence of carbide was more intense at 1200°C. Additionally, a higher I_{2D}/I_G ratio (0.418) was observed at 1200°C, which implies that there are fewer graphene layers at this temperature. The lowest I_D/I_G ratio (0.908) for the graphene layers was obtained at 1200°C, suggesting that graphene had fewer defects at this temperature. The size of the graphene domains was also calculated. We found that by increasing the growth temperature, the graphene domain size also increased.

Key words: chemical vapor deposition, Raman, graphene, molybdenum, growth temperature

1. Introduction

Graphene consists of a 2D hexagonal network of carbon atoms with a honeycomb structure. This material has attracted the interest of many scientists due to its desirable characteristics, including its excellent chemical inertness, atomic smoothness, high mechanical stability, high carrier mobility, current capabilities, and thermal conductivity [1-4]. A variety of methods have been used to prepare graphene, such as mechanical exfoliation of graphite, epitaxial growth on SiC, reduction of graphene oxide, unzipping of carbon nanotubes (CNTs), and chemical vapor deposition (CVD). Among these methods, CVD has emerged as the most commonly used approach for single and few-layer graphene syntheses on metal substrates. This method is particularly appealing because it is the most scalable and inexpensive deposition technique [5,6]. Graphene has been deposited via CVD on different transition metals (e.g., Pt [7], Pd [8], Re [9], Ni [10], Cu [3], Ru [11], Ir [12], Co [13], Rh [14], and W [15]), but very few groups have investigated the role of molybdenum (Mo) as a catalyst for graphene synthesis, despite that early studies showed that Mo may act as an effective catalyst for CNTs [16]. Also, using CVD, iron-Mo can act as a very efficient catalyst for the synthesis of single-walled and multi-walled CNTs [17]. However, the use of Mo as a catalyst for the production of graphene is still a new challenge. Wu et al. [18] reported the synthesis of large-area graphene on Mo foils by using CVD. They reported that the cooling rate can be used to control the number of graphene layers. Grachova et al. [19] reported the CVD of graphene onto sputtered thin-films of Mo. Hsieh et al. [20] studied the effects of the addition of Mo on the growth rate of graphene on Cu. They found that Mo affected the graphene quality

and increased the growth rate of graphene. As a catalyst, the high melting point, low thermal expansion, and surface smoothness of Mo help to create excellent conditions for the synthesis of high-quality graphene [19]. In the CVD method, the formation of graphene islands on the metal catalyst surface is the first step of the growth process. The formation of graphene islands is affected by a variety of factors, including the processing temperature, carbon affinity of the catalyst, carbon source, etc. The growth temperature has a direct effect on the formation and quality of the graphene and depends on the melting point of the metal catalyst. Vlassiouk et al. [21] investigated the effect of the growth temperature on the quality of graphene layers deposited by CVD on Cu foil. They reported that, in order to synthesize large single crystal graphene, the temperature should be near the melting point of Cu. Li et al. [22] reported the CVD of graphene on Cu foils at low temperatures by using hydrocarbon sources at a growth temperature as low as 400°C. Numerous studies have been carried out with Cu and Ni, showing that the best temperature for the deposition of graphene is 1000°C [23]. However, for Mo, finding the optimum temperature for the synthesis of high-quality graphene is still a challenge. In previous works that have used Mo foil, this temperature (1000°C) has typically been used [18,19].

In this research, graphene layers are synthesized on Mo foils by the CVD method. The quality and the number of layers are controlled by changing the growth temperature. To find the best growth temperature, samples were grown at 1000°C, 1100°C, and 1200°C.

2. Experimental

2.1. Materials and preparation

Reaction gases of hydrogen (H_2, 99.999%), argon (Ar, 99.999%), and methane (CH_4, with 99.995% purity) were purchased from A-Rang Gas Korea (Gwangmyeong, Korea). A 0.25-mm-thick annealed uncoated 99.95% pure Mo foil was purchased from Alfa Aesar (Ward Hill, MA, USA). Automated thermal CVD equipment from Scientific Engineers (Seoul, Korea) was utilized to deposit graphene on the Mo foil.

Graphene was grown by the CVD of CH_4 on Mo foils (1 × 1 cm^2). First, Mo foils were immersed in 1 M acetic acid at room temperature for 10 min. This was followed by immersion in acetone (10 min) and ethanol (10 min). The Mo foils were then put into a quartz tube furnace and exposed to H_2/Ar (200 and 500 sccm, respectively) at room pressure while the temperature was increased to the growth temperature. The quartz tube was held at the growth temperature (sample 1 at 1000°C, sample 2 at 1100°C, and sample 3 at 1200°C) for 10 min to remove any oxide layer on the Mo. The samples were then exposed to a CH_4/H_2/Ar gas mixture (100, 200, and 500 sccm, respectively) for 5 min, and then the furnace was cooled to room temperature (40°C/min cooling rate). The gas mixture used during the cooling process was the same as that used during the heating step.

2.2. Characterization

The crystal structures of the samples were investigated using X-ray diffraction (XRD) (D8 Advance; Bruker, Cu $K_{\alpha 1}$ [λ = 1.5406 Å]). X-ray photoelectron spectroscopy (XPS) measurements were performed using a K-Alpha System spectrometer (Thermo Electron, Waltham, MA, USA) equipped with an Al K_α monochromatic X-ray source (1486.7 eV) and a micro-focused monochromator. The qualities of the obtained graphene on Mo foils were investigated using Raman spectroscopy (RFS 100/S, Bruker; λ = 532 nm)

3. Results and Discussion

3.1. X-ray diffraction

Fig. 1 shows the XRD results of the Mo foils before any processing (bare sample) and also after graphene deposition at different temperatures. For bare samples, three peaks were located at 40.5°, 58.6°, and 73.7°. These correspond to the 110, 200, and 211 crystalline planes of Mo (JPCDS 89-5023), respectively. The diagram also shows the polycrystalline structure on the Mo foils.

In Fig. 1, graphs 1, 2, and 3 show the XRD patterns of the Mo foils after deposition at different growth temperatures. The presence of Mo_2C (carbide phase) peaks at 39.59° (101) and 52.31° (102) and the disappearance of Mo (110) indicate the presence of carbon atoms on the structure of the Mo foils as well as the precipitation of carbon onto the Mo surface [24]. The formation of carbide on the surface of Mo foils serves as an obstacle for the diffusion of more carbon onto the Mo surface; therefore, the deposited graphene is more uniform [18]. By comparing the XRD patterns of samples, it can be seen that the Mo_2C peaks of sample 3 (at 1200°C) have an increased intensity compared to the other samples. This is attributed to the solubility of carbon in the metal increasing as the temperature increases [25]. Therefore, at higher growth temperatures, more carbon precipitates on the metal surface (sample 3). Consequently, the graphene layer on this sample is of superior quality compared to the other samples [24].

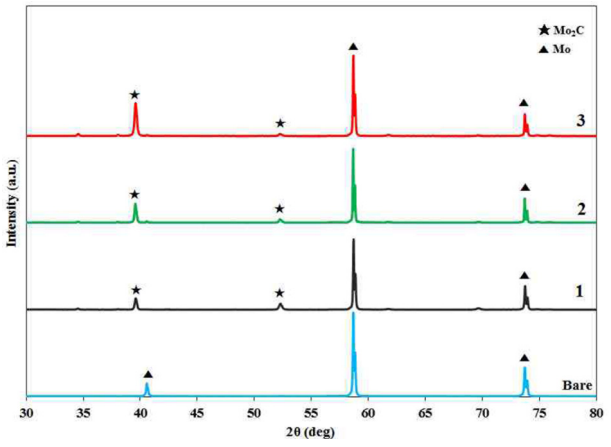

Fig. 1. X-ray diffraction patterns of the molybdenum (Mo) foils before growth and after graphene deposition at different temperatures.

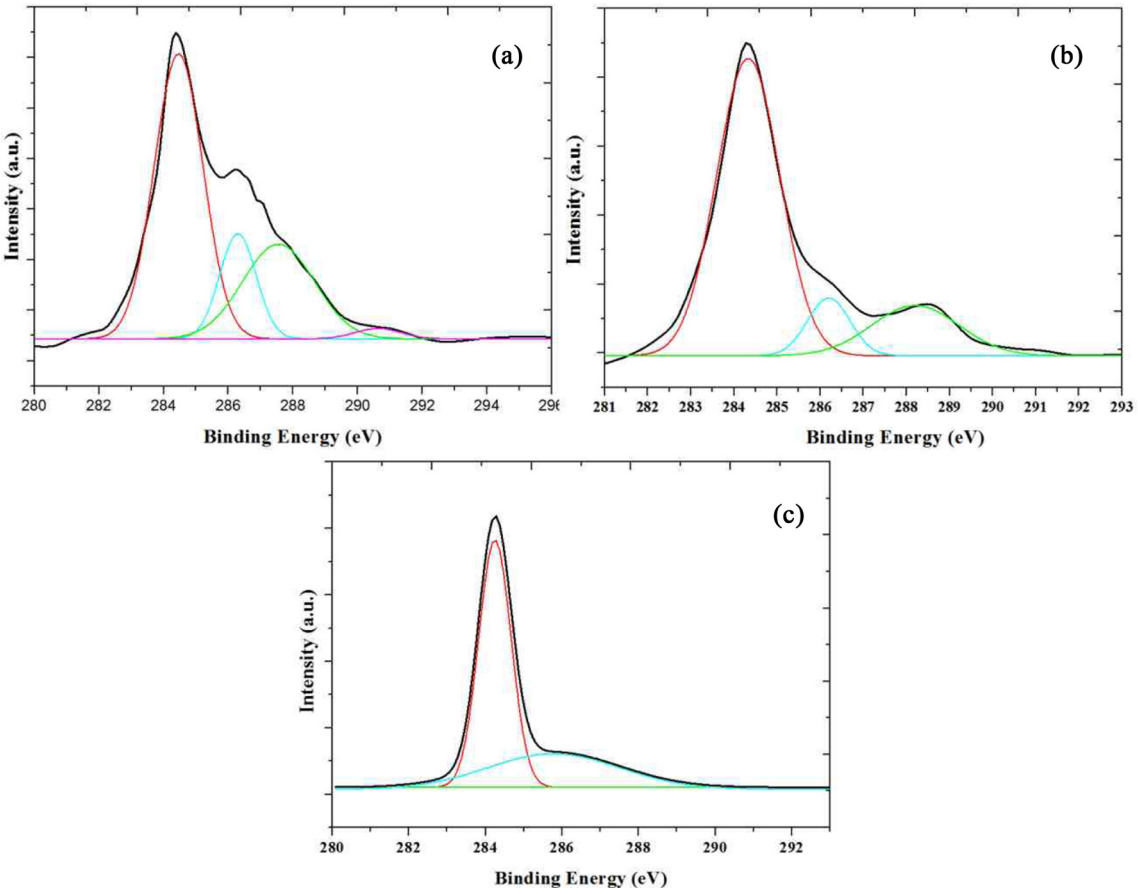

Fig. 2. C1s spectrum of graphene coated-molybdenum (Mo) foils: (a) sample 1, (b) sample 2, and (c) sample.3.

3.2. X-ray photoelectron spectroscopy

XPS was used to characterize the chemical bonds of the samples. Fig. 2 exhibits the C1s XPS spectra for the obtained samples. Fig. 2a shows the C1s spectrum of sample 1; two peaks are observable, which can be decomposed into four Gaussian peaks that correspond to carbon atoms in different functional groups at 284.5 eV (graphitic sp2 carbon), 286.3 eV (C-OH [hydroxyl]), 287.5 eV (C=O [carbonyl]), and 290.6 eV (O-C=O [carboxylate carbon]). Similarly, for sample 2, there were two peaks. These can be decomposed into three Gaussian peaks at 284.4 eV (graphitic sp2 carbon), 286.4 eV (C-OH [hydroxyl]), and 288.3 eV (C=O [carbonyl]). Fig. 2c shows the C1s spectrum of sample 3. Only one peak was observed, which corresponds to two Gaussian peaks centered at 284.2 eV (graphitic sp2 carbon) and 286.2 eV (C-OH [hydroxyl]). For all three samples, the strongest peak is observed around 284.6 eV, which indicates the good stability of the graphene coating [10,18,25].

The peak intensity of the sp2-hybridized C bonding for sample 3 is stronger than those of the other samples. Additionally, the estimated percentages of sp2-hybridized C atoms were 55.5%, 66.5%, and 69.1% for samples 1, 2, and 3, respectively (Table 1). This indicates that the obtained graphene coating of sample 3 has a high degree of graphitization. The appearance of oxygen functional groups (C-O and C=O) was caused by either the presence of oxygen atoms in the quartz tube furnace or by the absorption of oxygen by graphene after the samples were removed from the furnace [25].

Table 1. List of various carbon bonds and their percentages

Sample	C-C sp2 (%)	C-OH (%)	C=O (%)	O-C=O (%)
1	55.5	15.4	27.2	1.9
2	66.5	13.8	19.7	-
3	69.1	30.9	-	-

As can be seen in Fig. 2, when the temperature is increased, the C=C peak (around 284.4 eV) becomes larger and the peaks related to the oxygen functional groups (C-O, C=OH, and O-C=O) decrease or vanish completely. For nucleation of graphene on the metal catalyst surface, nucleation sites of the carbon must first form on the metal surface. This is followed by graphene growth. By increasing the temperature and limiting the lifetime of carbon at higher temperatures, some of these nucleation sites are destroyed. Therefore, due to the smaller number of sites, the graphene layer has fewer defects and better quality.

3.3. Raman spectroscopy

Fig. 3 shows the Raman spectra of graphene synthesized at different growth temperatures. Graphene typically has three prominent peaks in the Raman shift: the D band (at about 1350 cm^{-1}; related to defects in graphene layers), G band (at about 1582 cm^{-1}; related to the sp^2 carbon network and the number of graphene layers, where the intensity of the peak increases with more layers), and 2D band (at about 2700 cm^{-1}; related to the overtone of the D band, where the number of layers influences the peak positions and intensity of the 2D band, which decreases with more layers) [26]. Fig. 3 shows that the D peak is present in all samples. As mentioned earlier, the D band is related to defects in the graphene structure. Therefore, by calculating the intensity ratio between the D and G bands (I_D/I_G), the amount of defects can be calculated. Fig. 4a shows that I_D/I_G decreases with increasing growth temperature. Hence, at higher temperatures (1200°C) the graphene layers have fewer defects than the other samples. This result validates the XPS results. From Fig. 3, it is evident that the growth temperature has an influence on the number of graphene layers [21]. Additionally, the I_{2D}/I_G ratio is inversely proportional to the number of layers. Fig. 4b shows that I_{2D}/I_G decreases as the growth temperature increases. Therefore, it can be concluded that sample 3 (at 1200°C) has fewer graphene layers as compared to the other samples.

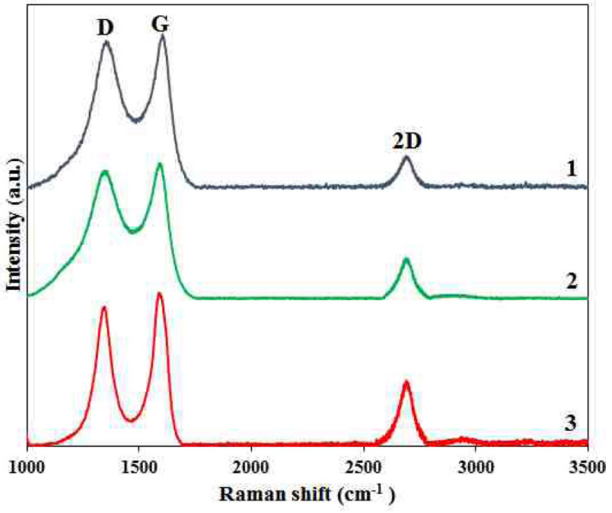

Fig. 3. Raman spectra of graphene grown at different growth temperatures from 1000°C to 1200°C.

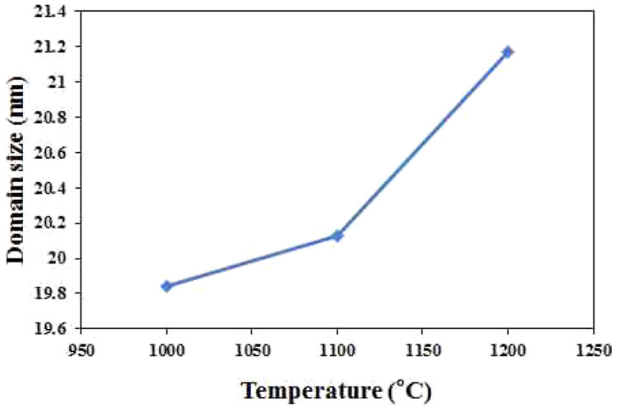

Fig. 5. Changes in L_α as a function of growth temperature.

By estimating the intensity ratio I_D/I_G, the graphene domain size can be calculated. This is done with the Tuinstra-Koenig relation [27]:

$$L_\alpha(nm) = (2.4 \times 10^{-10})\lambda_{laser}^4 (I_D/I_G)^{-1} \quad (1)$$

where, λ_{laser} is the excitation laser wavelength (λ_{laser} = 532 nm) and L_α is the crystallite size of the samples. L_α is calculated for all three samples; Fig. 5 shows that this is proportional to the growth temperature. The intensity ratio I_D/I_G is related to the defects in the graphene layers. As mentioned earlier, the amount of defects decreases as the growth temperature increases; higher growth temperatures lead to fewer defects and larger domains.

4. Conclusions

In this work, graphene was grown on Mo foil by CVD method at different growth temperatures (1000°C, 1100°C, and 1200°C). The deposited layers were investigated by XRD, XPS,

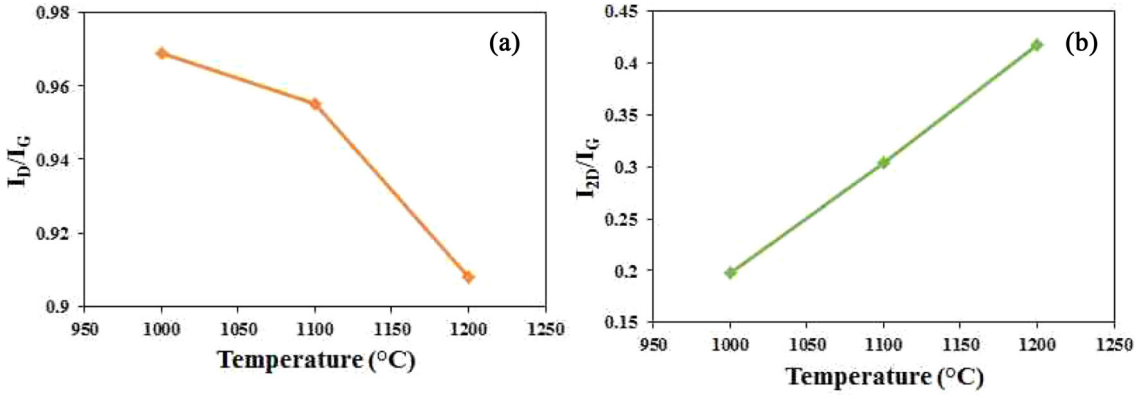

Fig. 4. Changes in (a) the I_D/I_G ratio and (b) the I_{2D}/I_G ratio as a function of growth temperature.

and Raman spectroscopy. The results showed that the quality of the deposited graphene layers is affected by the growth temperature. As the growth temperature increases, the number of graphene layers and the number of defects related to the layers both decrease. It was also found that increasing the growth temperature increases the graphene domain size.

Conflict of Interest

No potential conflict of interest relevant to this article was reported.

Acknowledgements

This work was supported by the Carbon Valley Project of the Ministry of Trade, Industry and Energy, South Korea

References

[1] Wang H, Xie G, Fang M, Ying Z, Tong Y, Zeng Y. Electrical and mechanical properties of antistatic PVC films containing multilayer graphene. Compos Part B: Eng, **79**, 444 (2015). http://dx.doi.org/10.1016/j.compositesb.2015.05.011.

[2] Naghdi S, Rhee KY, Jaleh B, Park SJ. Altering the structure and properties of iron oxide nanoparticles and graphene oxide/iron oxide composites by urea. Appl Surf Sci, **364**, 686 (2016). http://dx.doi.org/10.1016/j.apsusc.2015.12.225.

[3] Gan L, Shang S, Yuen CWM, Jiang SX, Luo NM. Facile preparation of graphene nanoribbon filled silicone rubber nanocomposite with improved thermal and mechanical properties. Compos Part B: Eng, **69**, 237 (2015). http://dx.doi.org/10.1016/j.compositesb.2014.10.019.

[4] Guermoune A, Chari T, Popescu F, Sabri SS, Guillemette J, Skulason HS, Szkopek T, Siaj M. Chemical vapor deposition synthesis of graphene on copper with methanol, ethanol, and propanol precursors. Carbon, **49**, 4204 (2011). http://dx.doi.org/10.1016/j.carbon.2011.05.054.

[5] Mattevi C, Kim H, Chhowalla M. A review of chemical vapour deposition of graphene on copper. J Mater Chem, **21**, 3324 (2011). http://dx.doi.org/10.1039/C0JM02126A.

[6] Mišković-Stanković V, Jevremović I, Jung I, Rhee KY. Electrochemical study of corrosion behavior of graphene coatings on copper and aluminum in a chloride solution. Carbon, **75**, 335 (2014). http://dx.doi.org/10.1016/j.carbon.2014.04.012.

[7] Cushing GW, Johánek V, Navin JK, Harrison I. Graphene growth on Pt(111) by ethylene chemical vapor deposition at surface temperatures near 1000 K. J Phys Chem C, **119**, 4759 (2015). http://dx.doi.org/10.1021/jp508177k.

[8] An X, Liu F, Jung YJ, Kar S. Large-area synthesis of graphene on palladium and their Raman spectroscopy. J Phys Chem C, **116**, 16412 (2012). http://dx.doi.org/10.1021/jp301196u.

[9] Tonnoir C, Kimouche A, Coraux J, Magaud L, Delsol B, Gilles B, Chapelier C. Induced superconductivity in graphene grown on rhenium. Phys Rev Lett, 111, 246805 (2013). http://dx.doi.org/10.1103/physrevlett.111.246805.

[10] Nayak PK, Hsu CJ, Wang SC, Sung JC, Huang JL. Graphene coated Ni films: a protective coating. Thin Solid Films, 529, 312 (2013). http://dx.doi.org/10.1016/j.tsf.2012.03.067.

[11] Sutter PW, Flege JI, Sutter EA. Epitaxial graphene on ruthenium. Nat Mater, 7, 406 (2008). http://dx.doi.org/10.1038/nmat2166.

[12] Vo-Van C, Kimouche A, Reserbat-Plantey A, Fruchart O, Bayle-Guillemaud P, Bendiab N, Coraux J. Epitaxial graphene prepared by chemical vapor deposition on single crystal thin iridium films on sapphire. Appl Phys Lett, 98, 181903 (2011). http://dx.doi.org/10.1063/1.3585126.

[13] Ago H, Ito Y, Mizuta N, Yoshida K, Hu B, Orofeo CM, Tsuji M, Ikeda KI, Mizuno S. Epitaxial chemical vapor deposition growth of single-layer graphene over cobalt film crystallized on sapphire. ACS Nano, 4, 7407 (2010). http://dx.doi.org/10.1021/nn102519b.

[14] Gotterbarm K, Zhao W, Höfert O, Gleichweit C, Papp C, Steinrück HP. Growth and oxidation of graphene on Rh(111). Phys Chem Chem Phys, **15**, 19625 (2013). http://dx.doi.org/10.1039/c3cp53802h.

[15] Zou Z, Song X, Chen K, Ji Q, Zhang Y, Liu Z. Uniform single-layer graphene growth on recyclable tungsten foils. Nano Res, **8**, 592 (2015). http://dx.doi.org/10.1007/s12274-015-0727-9.

[16] Park YS, Moon HS, Huh M, Kim BJ, Kuk YS, Kang SJ, Lee SH, An KH. Synthesis of aligned and length-controlled carbon nanotubes by chemical vapor deposition. Carbon Lett, **14**, 99 (2013). http://dx.doi.org/10.5714/cl.2013.14.2.099.

[17] Jodin L, Dupuis AC, Rouvière E, Reiss P. Influence of the catalyst type on the growth of carbon nanotubes via methane chemical vapor deposition. J Phys Chem B, **110**, 7328 (2006). http://dx.doi.org/10.1021/jp056793z.

[18] Wu Y, Yu G, Wang H, Wang B, Chen Z, Zhang Y, Wang B, Shi X, Xie X, Jin Z, Liu X. Synthesis of large-area graphene on molybdenum foils by chemical vapor deposition. Carbon, **50**, 5226 (2012). http://dx.doi.org/10.1016/j.carbon.2012.07.007.

[19] Grachova Y, Vollebregt S, Lacaita AL, Sarro PM. High quality wafer-scale CVD graphene on molybdenum thin film for sensing application. Procedia Eng, **87**, 1501 (2014). http://dx.doi.org/10.1016/j.proeng.2014.11.583.

[20] Hsieh YP, Hofmann M, Kong J. Promoter-assisted chemical vapor deposition of graphene. Carbon, **67**, 417 (2014). http://dx.doi.org/10.1016/j.carbon.2013.10.013.

[21] Vlassiouk I, Smirnov S, Regmi M, Surwade SP, Srivastava N, Feenstra R, Eres G, Parish C, Lavrik N, Datskos P, Dai S, Fulvio P. Graphene nucleation density on copper: fundamental role of background pressure. J Phys Chem C, **117**, 18919 (2013). http://dx.doi.org/10.1021/jp4047648.

[22] Li Z, Wu P, Wang C, Fan X, Zhang W, Zhai X, Zeng C, Li Z, Yang J, Hou J. Low-temperature growth of graphene by chemical vapor deposition using solid and liquid carbon sources. ACS Nano, **5**, 3385 (2011). http://dx.doi.org/10.1021/nn200854p.

[23] Li X, Magnuson CW, Venugopal A, An J, Suk JW, Han B, Borysiak M, Cai W, Velamakanni A, Zhu Y, Fu L, Vogel EM, Voelkl E, Colombo L, Ruoff RS. Graphene films with large domain size by a two-step chemical vapor deposition process. Nano Lett, **10**, 4328 (2010). http://dx.doi.org/10.1021/nl101629g.

[24] Chen Y, Zhang H, Zhang J, Ma J, Ye H, Qian G, Ye Y, Zhong S. Facile synthesis and thermal stability of nanocrystalline molybdenum carbide. Mater Sci Appl, **2**, 1313 (2011). http://dx.doi.org/10.4236/msa.2011.29178.

[25] Jourdain V, Bichara C. Current understanding of the growth of carbon nanotubes in catalytic chemical vapour deposition. Carbon, **58**,

2 (2013). http://dx.doi.org/10.1016/j.carbon.2013.02.046.

[26] Son YR, Rhee KY, Park SJ. Influence of reduced graphene oxide on mechanical behaviors of sodium carboxymethyl cellulose. Compos Part B: Eng, **83**, 36 (2015). http://dx.doi.org/10.1016/j.compositesb.2015.08.031.

[27] Cançado LG, Takai K, Enoki T, Endo M, Kim YA, Mizusaki H, Jorio A, Coelho LN, Magalhães-Paniago R, Pimenta MA. General equation for the determination of the crystallite size L_a of nanographite by Raman spectroscopy. Appl Phys Lett, **88**, 163106 (2006). http://dx.doi.org/10.1063/1.2196057.